Real and Complex Variable Models of Potential Flow

Bryce D. Wilkins[1],
Saleem Ali[2],
Sebastian Neumann[2],
Theodore V. Hromadka II[3]

[1]Columbia University
[2]United States Military Academy
[3]Distinguished Professor, United States Military Academy

November 22, 2022

Bryce D. Wilkins[1], Saleem Ali[2], Sebastian Neumann[2], Theodore V. Hromadka II[3]
Corresponding Author: Bryce D. Wilkins, bdw2126@columbia.edu

Section 1

Methodologies

Bryce D. Wilkins[1], Saleem Ali[2], Sebastian Neumann[2], Theodore V. Hromadka II[3]
Corresponding Author: Bryce D. Wilkins, bdw2126@columbia.edu

Real and Complex Variable Models

Method of Fundamental Solutions

$$g_{\text{rv}}(\boldsymbol{x}, \boldsymbol{x}') = -\frac{1}{2\pi} \log |\boldsymbol{x} - \boldsymbol{x}'|$$

$$\hat{\phi}_{\text{rv}}(\boldsymbol{x}) = \sum_{j=1}^{n} a_j \log |\boldsymbol{x} - \boldsymbol{x}'|, \; a_j \in \mathbb{R}$$

where $\boldsymbol{x} = \begin{bmatrix} x \\ y \end{bmatrix}$

Complex Variable Simple Pole Approach

$$g_{\text{cv}}(z, z') = \frac{1}{z - z'}$$

$$\hat{\phi}_{\text{cv}}(\boldsymbol{x}) = \Re \left[\sum_{j=1}^{n} \frac{c_j}{z - z_j} \right], \; c_j \in \mathbb{C}$$

where $z = x + iy$

Bryce D. Wilkins[1], Saleem Ali[2], Sebastian Neumann[2], Theodore V. Hromadka II[3]
Corresponding Author: Bryce D. Wilkins, bdw2126@columbia.edu

The General CVBEM Approximation Function

- The CVBEM approximation function is a linear combination of complex variable functions that are analytic within a given problem domain, Ω:

$$\hat{\omega}(z) = \sum_{j=1}^{n} c_j g_j(z), \quad z \in \Omega, \tag{1}$$

- where
  - $c_j = \alpha_j + i\beta_j$ are complex coefficients,
  - $g_j(z)$ are analytic complex variable basis functions,
  - n is the number of basis functions being used in the approximation
- In the collocation approach, each term in the approximation function corresponds to one node and two collocation points.

Some possible basis functions:

- $(z - z_j)\ln_{\alpha_j}(z - z_j)$
- $1/(z - z_j)$
- $(z - z_j)^j$
- Digamma
- Polygamma
- And more!

Hromadka II, T.V., Guymon, G.L., A Complex Variable Boundary Element Method: Development. *International Journal for Numerical Methods in Engineering*, pp. 25-37, 1984.

Bryce D. Wilkins[1], Saleem Ali[2], Sebastian Neumann[2], Theodore V. Hromadka II[3]
Corresponding Author: Bryce D. Wilkins, bdw2126@columbia.edu

Node Position Algorithm (NPA)

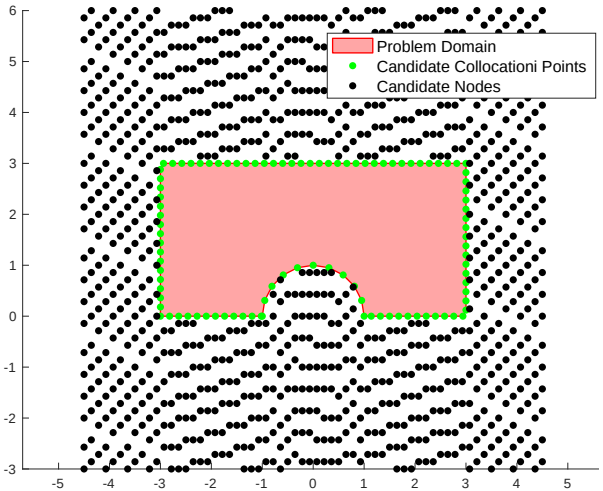

Figure: Candidate nodes are tested one-at-a-time to determine which node contributes the most to reducing the maximum error of the MFS or CVBEM approximation function.

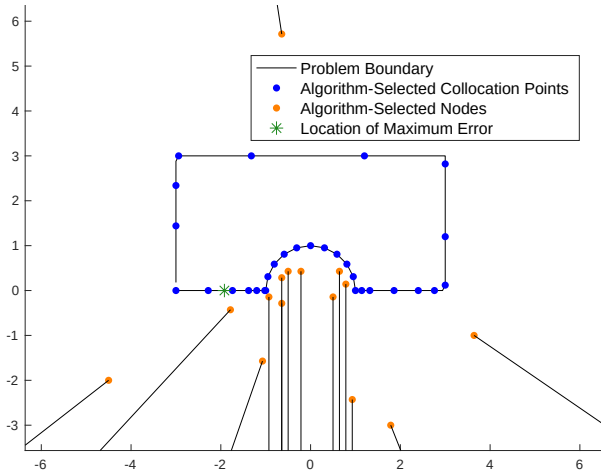

Figure: After a node is selected, the maximum error of the resulting CVBEM model is assessed. Two new collocation points are added at the two highest local maxima of the error function.

Demoes, N.J., Bann, G.T., Wilkins, B.D., Grubaugh, K.E. & Hromadka II, T.V., Optimization Algorithm for Locating Computational Nodal Points in the Method of Fundamental Solutions to Improve Computational Accuracy in Geosciences Modeling. *The Professional Geologist*, pp. 6-12, 2019.

Bryce D. Wilkins[1], Saleem Ali[2], Sebastian Neumann[2], Theodore V. Hromadka II[3]
Corresponding Author: Bryce D. Wilkins, bdw2126@columbia.edu

Error Computation

- The maximum principle of harmonic functions states that the maximum value of a harmonic function restricted to a particular domain occurs on the boundary of that domain.
- Let Ω denote the problem domain. Our basis functions are constructed to be harmonic in Ω. The target function is harmonic in Ω. Therefore, $\phi - \hat{\phi}$ is harmonic in Ω.
- Thus, $\max_{(x,y)\in\bar{\Omega}} |\phi - \hat{\phi}| = \max_{(x,y)\in\partial\Omega} |\phi - \hat{\phi}|$

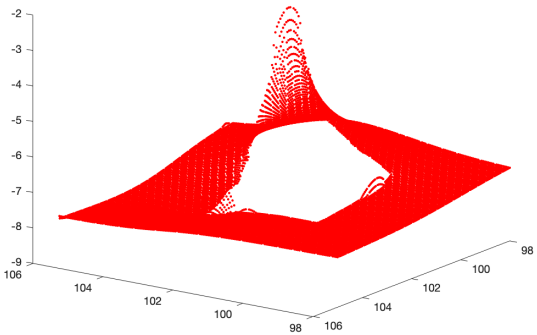

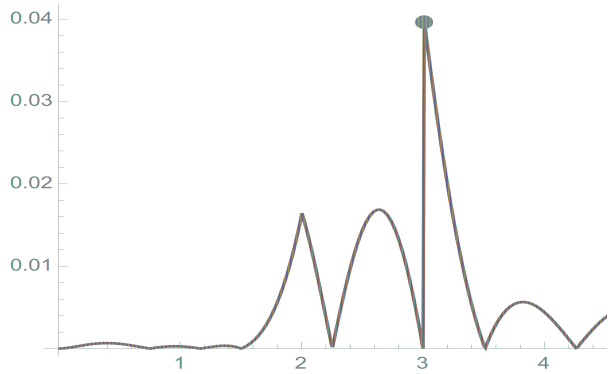

Bryce D. Wilkins[1], Saleem Ali[2], Sebastian Neumann[2], Theodore V. Hromadka II[3]
Corresponding Author: Bryce D. Wilkins, bdw2126@columbia.edu

Handling Mixed Boundary Conditions

The Dirichlet boundary conditions:

$$\begin{aligned}\hat{\phi}(x_{i,\mathrm{D}}, y_{i,\mathrm{D}}) &= \sum_{j=1}^{n} \alpha_j \lambda_j(x_{i,\mathrm{D}}, y_{i,\mathrm{D}}) - \beta_j \mu_j(x_{i,\mathrm{D}}, y_{i,\mathrm{D}}) \\ &= \phi(x_{i,\mathrm{D}}, y_{i,\mathrm{D}}), \\ &\text{for } \; i = 1, \ldots, N_{\mathrm{D}}, \quad (x_{i,\mathrm{D}}, y_{i,\mathrm{D}}) \in \partial\Omega_{\mathrm{D}}.\end{aligned}$$

The Neumann boundary conditions:

$$\begin{aligned}\hat{\psi}(x_{i,\mathrm{N}}, y_{i,\mathrm{N}}) &= \sum_{j=1}^{n} \alpha_j \mu_j(x_{i,\mathrm{N}}, y_{i,\mathrm{N}}) + \beta_j \lambda_j(x_{i,\mathrm{N}}, y_{i,\mathrm{N}}) \\ &= \text{const}, \\ &\text{for } \; i = 1, \ldots, N_{\mathrm{N}}, \quad (x_{i,\mathrm{N}}, y_{i,\mathrm{N}}) \in \partial\Omega_{\mathrm{N}}.\end{aligned}$$

Let:

$$\boldsymbol{x}_{\mathrm{D}} = \begin{bmatrix} x_{1,\mathrm{D}} \\ x_{2,\mathrm{D}} \\ \vdots \\ x_{N_{\mathrm{D}},\mathrm{D}} \end{bmatrix}, \quad \boldsymbol{y}_{\mathrm{D}} = \begin{bmatrix} y_{1,\mathrm{D}} \\ y_{2,\mathrm{D}} \\ \vdots \\ y_{N_{\mathrm{D}},\mathrm{D}} \end{bmatrix},$$

$$\boldsymbol{x}_{\mathrm{N}} = \begin{bmatrix} x_{1,\mathrm{N}} \\ x_{2,\mathrm{N}} \\ \vdots \\ x_{N_{\mathrm{N}},\mathrm{N}} \end{bmatrix}, \quad \text{and} \quad \boldsymbol{y}_{\mathrm{N}} = \begin{bmatrix} y_{1,\mathrm{N}} \\ y_{2,\mathrm{N}} \\ \vdots \\ y_{N_{\mathrm{N}},\mathrm{N}} \end{bmatrix}.$$

In matrix form:

$$\begin{bmatrix} \underbrace{\boldsymbol{\phi}(\boldsymbol{x}_{\mathrm{D}}, \boldsymbol{y}_{\mathrm{D}})}_{N_{\mathrm{D}} \times 1} \\ \underbrace{\boldsymbol{f}}_{N_{\mathrm{N}} \times 1} \end{bmatrix} = \begin{bmatrix} \underbrace{\lambda(\boldsymbol{x}_{\mathrm{D}}, \boldsymbol{y}_{\mathrm{D}})}_{N_{\mathrm{D}} \times n} & \underbrace{-\mu(\boldsymbol{x}_{\mathrm{D}}, \boldsymbol{y}_{\mathrm{D}})}_{N_{\mathrm{D}} \times n} \\ \underbrace{\mu(\boldsymbol{x}_{\mathrm{N}}, \boldsymbol{y}_{\mathrm{N}})}_{N_{\mathrm{N}} \times n} & \underbrace{\lambda(\boldsymbol{x}_{\mathrm{N}}, \boldsymbol{y}_{\mathrm{N}})}_{N_{\mathrm{N}} \times n} \end{bmatrix} \begin{bmatrix} \underbrace{\boldsymbol{\alpha}}_{n \times 1} \\ \underbrace{\boldsymbol{\beta}}_{n \times 1} \end{bmatrix},$$

where $\boldsymbol{f} = \gamma \begin{bmatrix} 1 \\ 1 \\ 1 \\ \vdots \\ 1 \end{bmatrix}, \quad \gamma \in \mathbb{R}.$

Bryce D. Wilkins[1], Saleem Ali[2], Sebastian Neumann[2], Theodore V. Hromadka II[3]
Corresponding Author: Bryce D. Wilkins, bdw2126@columbia.edu

Section 2

Example Problems and Results

Bryce D. Wilkins[1], Saleem Ali[2], Sebastian Neumann[2], Theodore V. Hromadka II[3]
Corresponding Author: Bryce D. Wilkins, bdw2126@columbia.edu

Corner Problem: Four Approaches

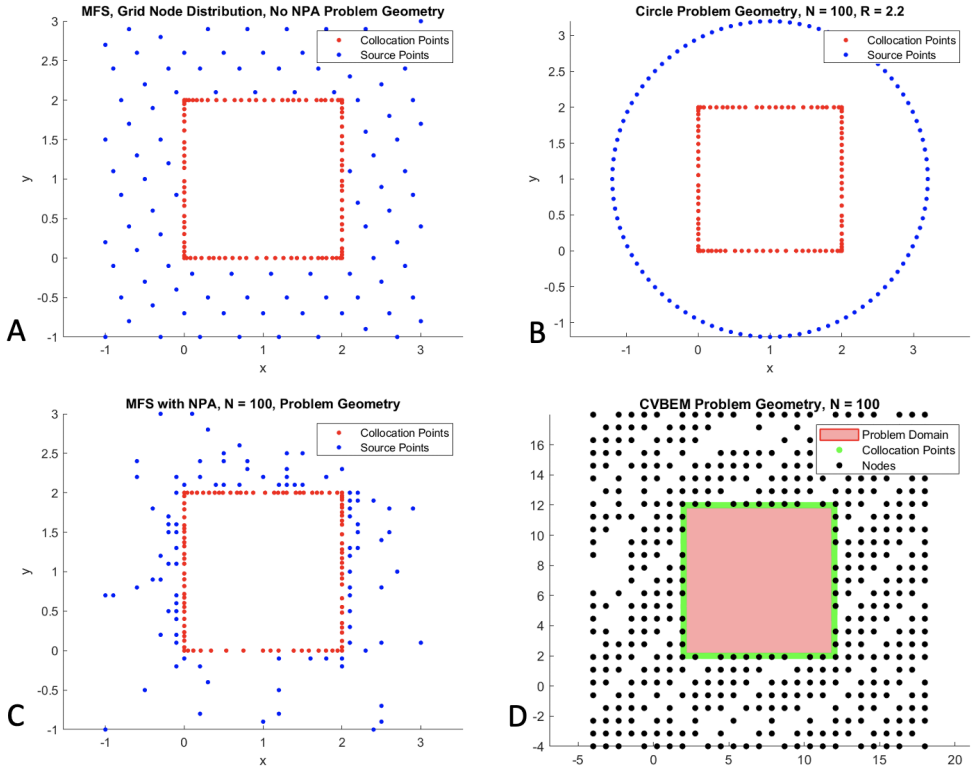

Figure: Problem geometry plots for the four different approaches. For all approaches, 100 nodes and collocations were used.

Bryce D. Wilkins[1], Saleem Ali[2], Sebastian Neumann[2], Theodore V. Hromadka II[3]
Corresponding Author: Bryce D. Wilkins, bdw2126@columbia.edu

Error Comparison

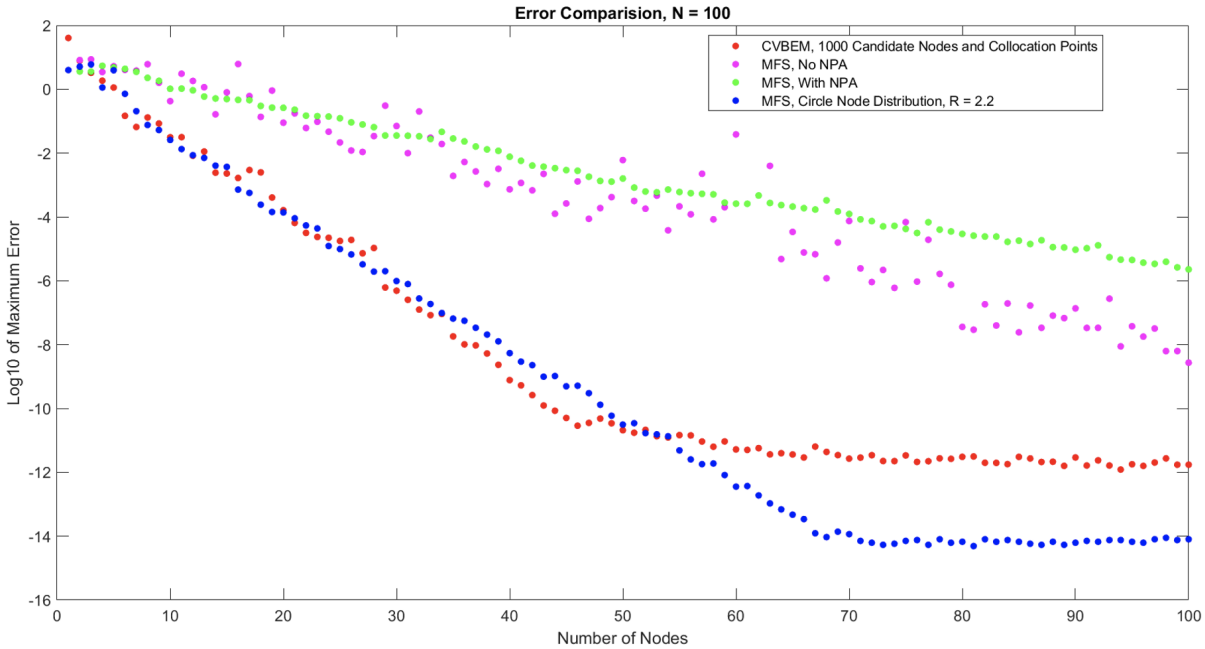

Figure: Comparison of the maximum error plots from CVBEM method and three different MFS methods. CVBEM outperforms the grid node distribution and MFS with the NPA, but the circle node distribution with optimized radius is able to outperform the CVBEM.

Bryce D. Wilkins[1], Saleem Ali[2], Sebastian Neumann[2], Theodore V. Hromadka II[3]
Corresponding Author: Bryce D. Wilkins, bdw2126@columbia.edu

Additional Results

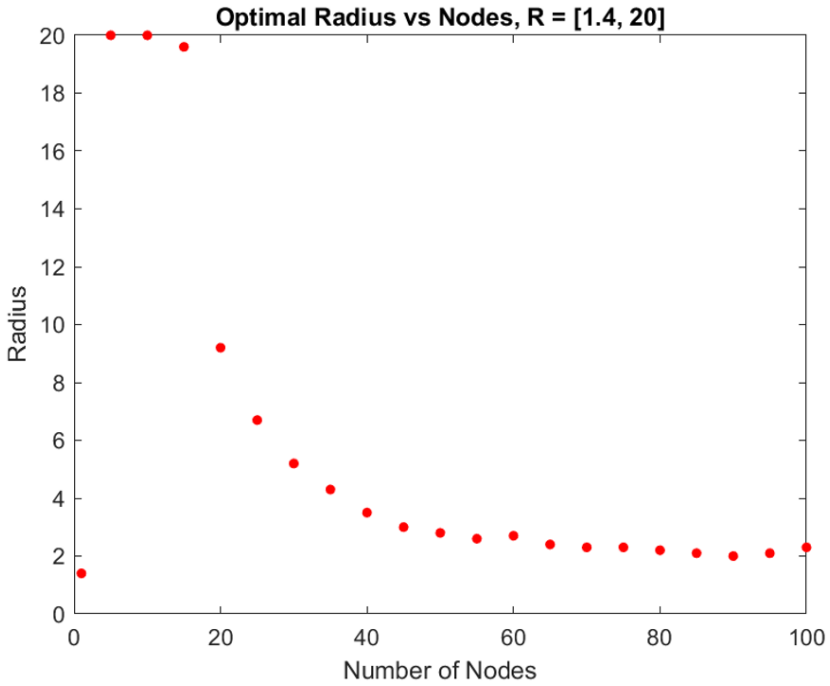

Figure: Optimal circle radius for up to $n = 100$ nodes.

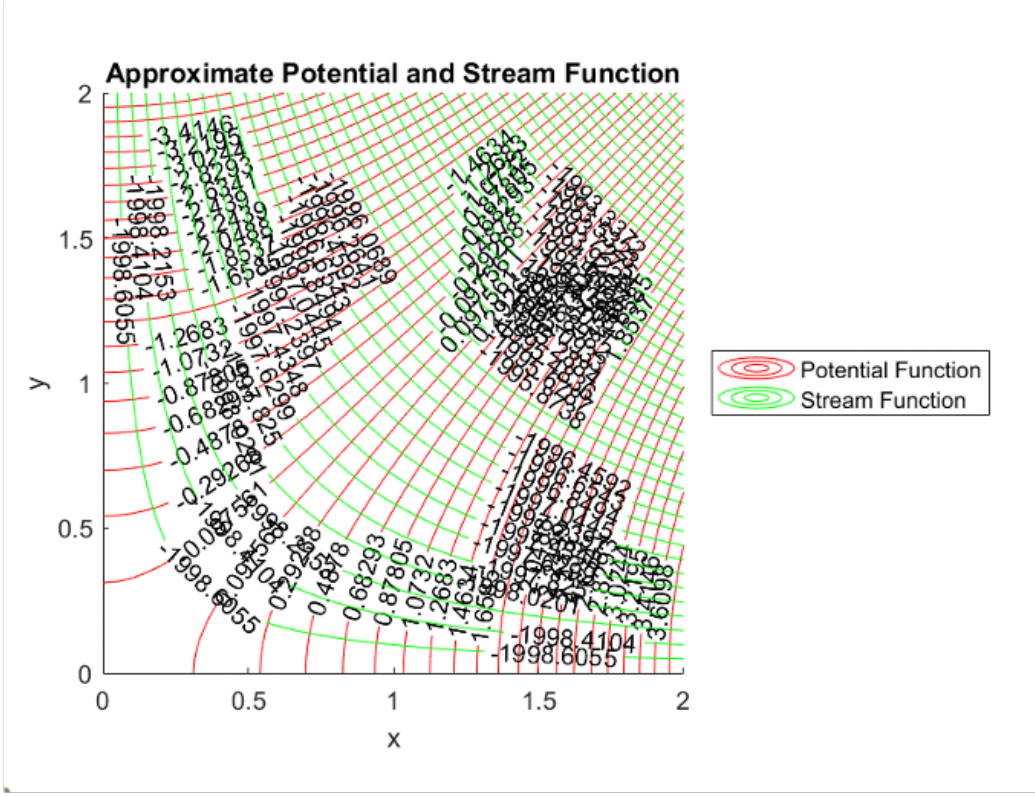

Figure: Approximate potential and stream functions for $n = 50$ nodes.

Bryce D. Wilkins[1], Saleem Ali[2], Sebastian Neumann[2], Theodore V. Hromadka II[3]
Corresponding Author: Bryce D. Wilkins, bdw2126@columbia.edu

NPA with Gaussian Randomness

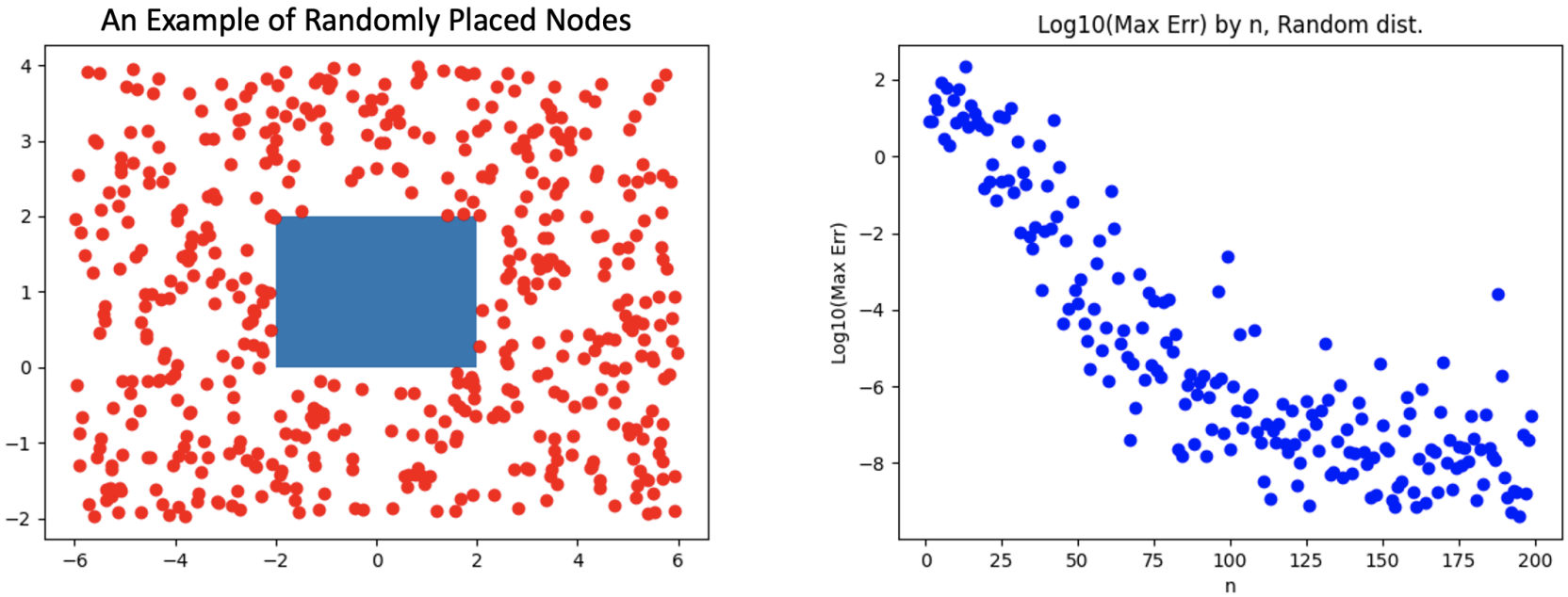

Figure: (Left) Sample distribution of candidate nodes with random placement. (Right) log_{10} of maximum error for various-sized MFS models.

Bryce D. Wilkins[1], Saleem Ali[2], Sebastian Neumann[2], Theodore V. Hromadka II[3]
Corresponding Author: Bryce D. Wilkins, bdw2126@columbia.edu

NPA with Gaussian Randomness - Radius Examination

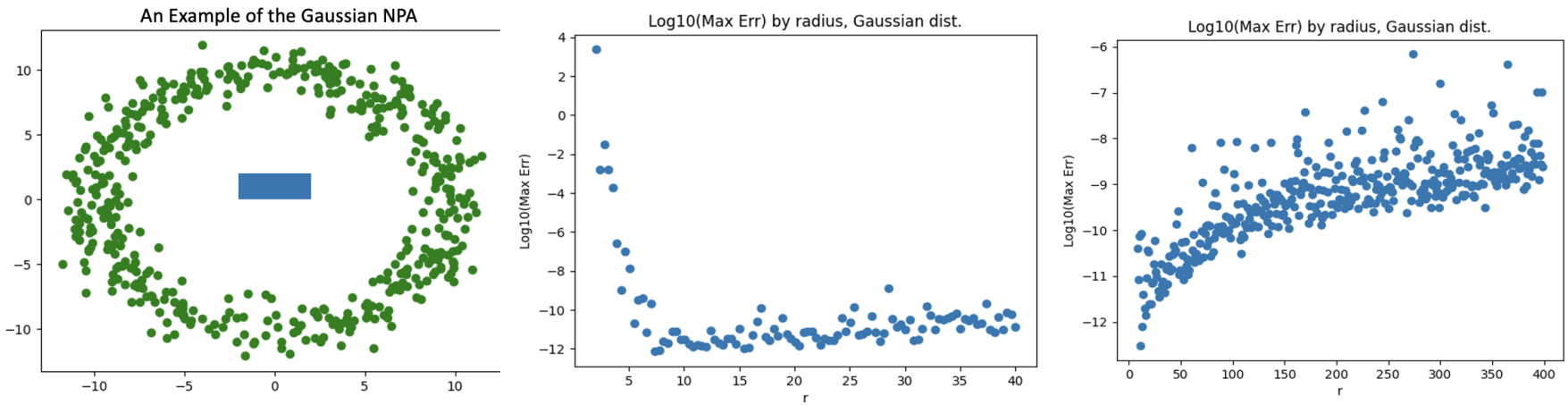

Figure: (Left) Sample distribution of candidate nodes at a specified radius with Gaussian randomness applied. (Center) log_{10} of maximum error for an MFS model as the radius of nodes is varied. Radii between 1 and 40 were examined. (Right) log_{10} of maximum error for an MFS model as the radius of nodes is varied. Radii between 1 and 400 were examined.

Bryce D. Wilkins[1], Saleem Ali[2], Sebastian Neumann[2], Theodore V. Hromadka II[3]
Corresponding Author: Bryce D. Wilkins, bdw2126@columbia.edu

Section 3

Final Thoughts - Upcoming Research

Bryce D. Wilkins[1], Saleem Ali[2], Sebastian Neumann[2], Theodore V. Hromadka II[3]
Corresponding Author: Bryce D. Wilkins, bdw2126@columbia.edu

Composite Approximation Function with Line-search NPA

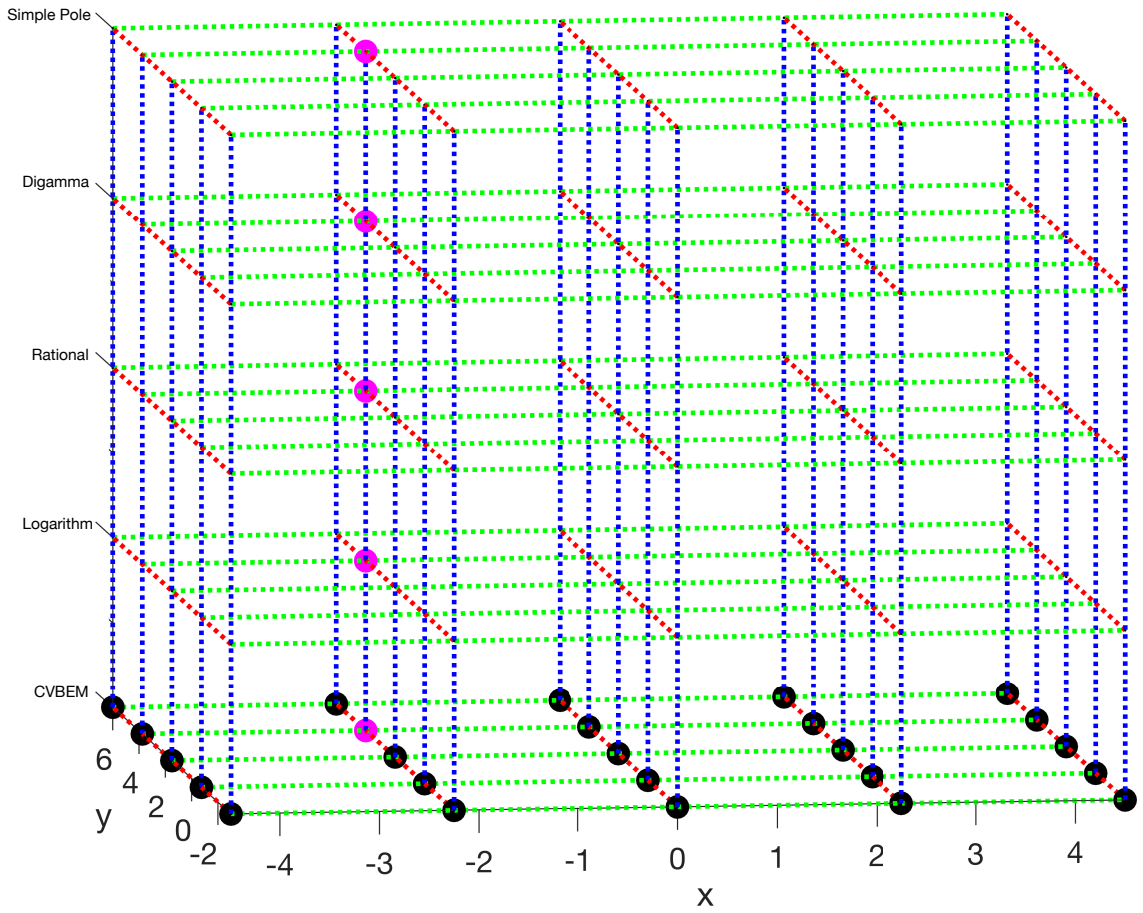

Figure: An alternative to the existing NPA is this algorithm, which proposes determining the location of each node, and then determining which basis function from a set of candidate functions to use at that particular location.

Bryce D. Wilkins[1], Saleem Ali[2], Sebastian Neumann[2], Theodore V. Hromadka II[3]
Corresponding Author: Bryce D. Wilkins, bdw2126@columbia.edu

Questions

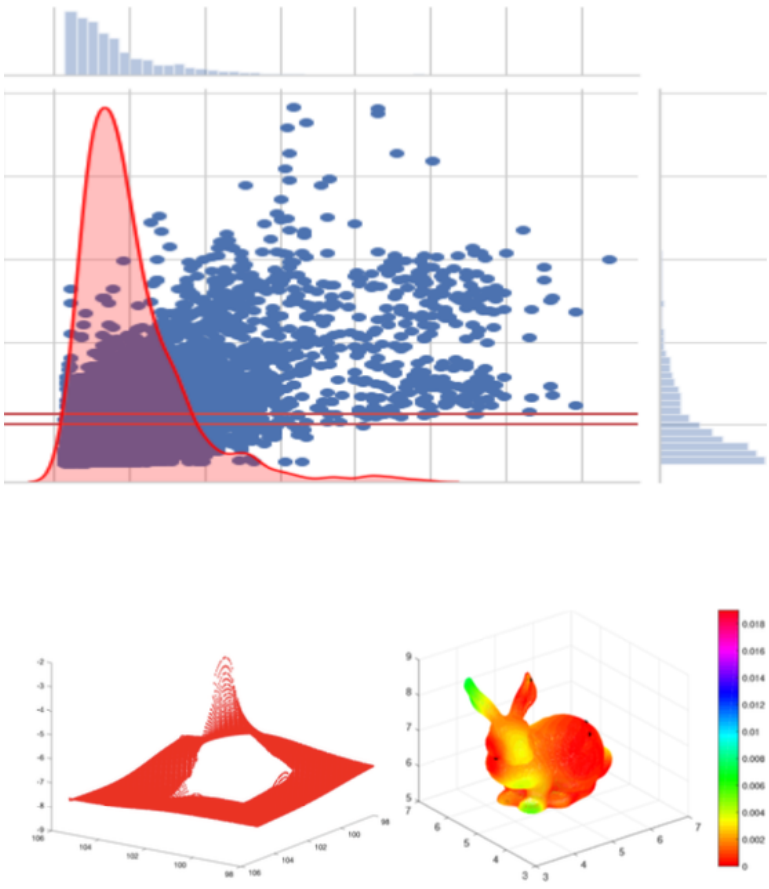

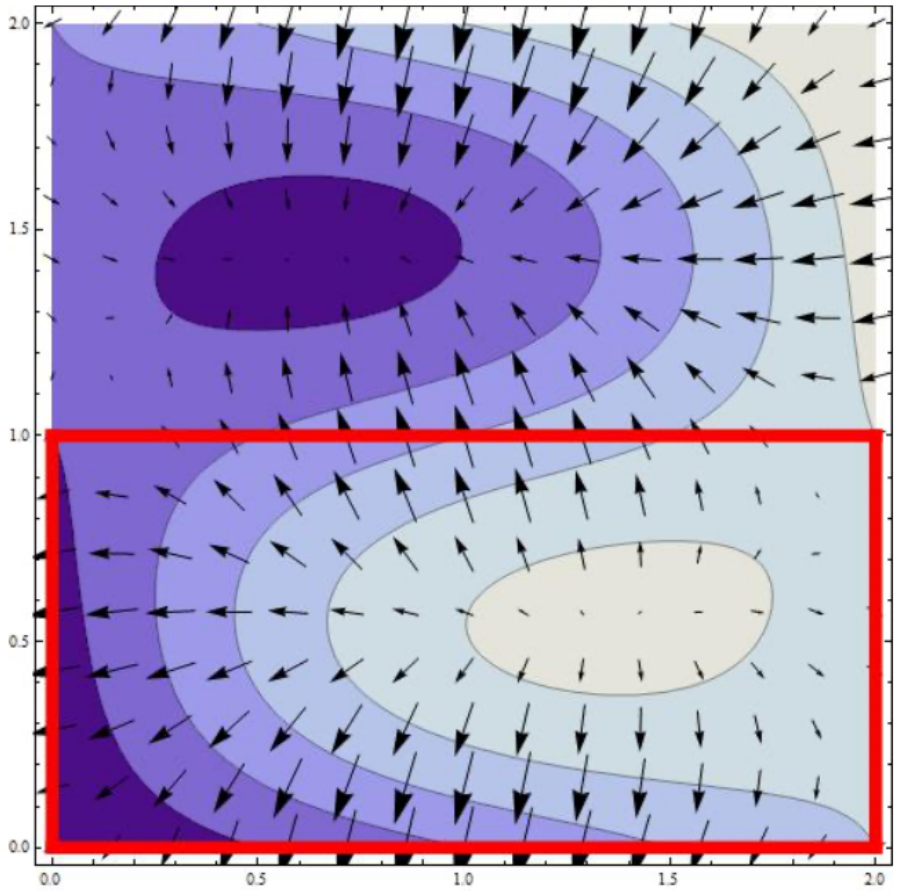

Bryce D. Wilkins[1], Saleem Ali[2], Sebastian Neumann[2], Theodore V. Hromadka II[3]
Corresponding Author: Bryce D. Wilkins, bdw2126@columbia.edu